Acta Polytechnica **53**(1):5–10, 2013

available online at `http://ctn.cvut.cz/ap/`

ON SOME STATISTICAL PROPERTIES OF GRBS WITH MEASURED REDSHIFTS HAVING PEAKS IN OPTICAL LIGHT CURVES

Grigorii Beskin[a,*], Giuseppe Greco[b], Gor Oganesyan[c], Sergey Karpov[a]

[a] *Special Astrophysical Observatory of Russian Academy of Sciences*

[b] *Astronomical Observatory of Bologna, INAF, Italy*

[c] *South Federal University, Russia*

[*] corresponding author: `beskin@sao.ru`

Abstract. We studied the subset of optical light curves of gamma-ray bursts with measured redshifts and well-sampled R band data that have clearly detected peaks. Among 43 such events, 11 are prompt optical peaks (P), coincident with gamma-ray activity, 22 are purely afterglows (A), and 10 more carry the signatures of an underlying activity (A(U)). We studied pair correlations of their gamma-ray and optical parameters, e.g. total energetics, peak optical luminosities, and durations. The main outcome of our study is the detection of source frame correlations between both optical peak luminosity and total energy and the redshift for classes A and A(U), and the absence of such a correlation for class P events. This result seems to provide evidence of the cosmological evolution of a medium around the burst defining class A and A(U) energetics, and the absence of cosmological evolution of the internal properties of GRB engines. We also discuss some other prominent correlations.

Keywords: gamma-ray bursts, statistical methods.

1. Introduction

The very first time when optical afterglows of GRBs were observed, it was immediately obvious that these phenomena are no mere extinguishing of the energy that powered GRBs, but rather, that they represent a vast wealth of physical phenomena that are not yet fully understood.

The aim of our work is to develop a statistical analysis of the prominent optical peaks that characterize several GRBs in the early stage of their emission. These are important for a study of the properties of the interstellar medium over a wide range of distances, and of the physical mechanisms operating during the transition phases between internal/external shock.

With this purpose in mind, we discuss the selection criteria and the classification scheme for the GRB sample with a well-measured optical peak. We study the correlations of pairs of parameters of these GRBs, and define possible directions for future work.

We adopt the concordance ΛCDM cosmology with $\Omega_{\rm M} = 0.3$, $\Omega_\Lambda = 0.7$, and $H_0 = 70\,{\rm km\,s^{-1}\,Mpc^{-1}}$.

2. Method and classification

We gathered all available GRBs with measured redshifts z and well sampled optical light curves that present a clear peak or peaks during its evolution (over the period from February 28, 1997 until February 28, 2011).

Subsequently, the entire optical peak sample was divided into sub-groups that took into account the main characteristics of the contemporaneous emissions at higher energies. In particular, we were interested in comparing the rising phases of optical emission with simultaneous behaviour at gamma-ray wavelengths, as observed by space-borne telescopes.

This operational classification leads to the division of our sample into three main sub-groups.

- **P**: optical peaks arise during the main phases of the prompt gamma-ray emission; we will refer to these as prompt optical emission.
- **A(U)**: there is still some residual underlying gamma-ray activity simultaneously with the formation of the optical peak.
- **A**: no significant gamma-ray activity is seen simultaneously with the onset of the optical peak
- **P?**: events that may not be unambiguously classified either as **A(U)** or as **P**. Three of the **P?** objects fall into the **A(U)**-populated regions of the correlation plots. We also use **P-3** notation to refer to all prompt events except **P?** events.

The observed optical peak flux $F_{\rm opt}$ was obtained using the calibration of [1]

$$F_{\rm opt} = 1568 \cdot \left(2.15 \cdot 10^{-9} \cdot 10^{-0.4{\rm mag}}\right) {\rm erg\,cm^{-2}\,s^{-1}} \quad (1)$$

and was then corrected for galactic extinction (based on the map of [2]) and for the brightness of the host galaxy (if this value is available). For the bursts whose the spectral index β and the host galaxy extinction $A_{\rm host}$ are not yet available, we assumed $\beta = 0.75$ and

the mean value of $A_{\rm host}$ measured in the corresponding ranges of the redshifts. Namely, the $A_{\rm host}$ data collected in the golden sample presented in [3] were divided into five redshift ranges and for each distance interval the corresponding average value of A_v was obtained.

The isotropic equivalent luminosity $L_{\rm opt}$ of the optical peak is related to the peak optical flux $F_{\rm opt}$ by

$$L_{\rm opt} = 4\pi\kappa_{\rm opt}(z)D_{\rm l}^2(z)F_{\rm opt}, \qquad (2)$$

where $D_l(z)$ is the luminosity distance for the standard cosmological model and $\kappa_{\rm opt}(z)$ is the cosmological κ-correction that takes into account the transformation of the R passband to the proper GRB rest frame:

$$\kappa_{\rm opt} = \left(\int\limits_{\frac{\nu R_0}{1+z}}^{\frac{\nu R_1}{1+z}} \nu^{-\beta} d\nu\right) \Big/ \left(\int\limits_{\nu R_0}^{\nu R_1} \nu^{-\beta} d\nu\right) = \frac{1}{(1+z)^{1-\beta}}, \qquad (3)$$

Here, νR_0 and νR_1 are the frequency boundaries of the R band and β is the power-law index of the optical spectrum $F_\nu \propto \nu^{-\beta}$.

The optical fluence $S_{\rm opt}$ was determined by numerical integration of the afterglow light curve over the interval from the earliest observation to the latest observation with a power-law interpolation of the flux $F(t)$ in the segments between the observational points. Since only a part of the optical afterglow light curve may be recorded in practice, this quantity is actually only a lower limit for the fluence.

The isotropic equivalent of the total optical energy in the R band $E_{\rm opt}$ in the rest frame of the source was determined from the optical fluence $S_{\rm opt}$ using the relation:

$$E_{\rm opt} = \frac{4\pi\kappa_{\rm opt}(z)D_l^2(z)S_{\rm opt}}{1+z}. \qquad (4)$$

Below is a list of quantities we use to characterize the GRBs.

The duration of the burst until the emission of 90 % of its energy, $t_{\rm opt}$; the delay of the maximal optical flux after the gamma-ray trigger, $t_{\rm peak}$; the width of the optical peak on the 10 % from the maximum, $t_{\rm width}$. These quantities are converted to the comoving frame by dividing by $(1+z)$, in the same way as the total fluences in the optical and gamma ranges (S_γ and $S_{\rm opt}$) are converted to the rest frame energies $E_{\rm iso}$ and $E_{\rm opt}$, also taking into account the *kappa*-correction. The shape of the optical light curves is characterized by the power-law indices of the rise before the peak and decay after the peak, $\alpha_{\rm r}$ and $\alpha_{\rm d}$. The peak optical and gamma light curve values are characterized by the fluxes F_γ and $F_{\rm opt}$, and also by the rest frame isotropic equivalent luminosities $L_{\rm iso}$ and $L_{\rm opt}$. Finally, the gamma-ray spectrum is characterized by the photon index α .

To measure the relations between different parameters we use unweighted Pearson correlation coefficient R, computed for the logarithms of all quantities. The significances of these estimates are computed using Student' t-distribution for the quantity $T = R\frac{\sqrt{n-2}}{\sqrt{1-R^2}}$, where n is the sample size.

3. Results

Table 1 lists all the pair correlations for various classes of optical companions with correlation coefficients greater than 0.5 and significances better than 1 %.

We found a strong correlation between the peak optical luminosity and the redshift for all object classes except for the prompt class (see the lower right panel of Figure 1). There ls a less obvious, but still significant, correlation of the optical energetics and the redshift. This may provide evidence for the cosmological evolution of interstellar medium parameters in regions around the progenitors of long gamma-ray bursts.

We detected significant connections between energies and peak luminosities, both in the gamma-ray range and in optical range, for all classes of objects (see the upper row of panels in Figure 1), and also between the optical energetics and the peak luminosities and energetics in gamma-rays. It is worth noting that in the latter cases the characteristics of these connections are similar in all classes. This suggests similar jet opening angles in gamma-ray and optical emission regions. In Table 2, we show the parameters of linear fits of quantities whose correlation coefficients are shown in bold in Table 1.

A detailed discussion of all detected correlations will be performed in the future.

4. Conclusions

Monitoring of robotic telescopes has helped us to understand some characteristics of optical emissions; from the region of peak formation, the gamma-ray emission can proceed in coincidence with the optical luminosity (P), can be extinguished (A), or can carry the remnants of an underlying activity (A(U)). In the case of A or A(U), the peak events that arise when prompt gamma-ray emission is completely extinguished appear to carry the signatures of the circumburst environment at different cosmological epochs. In the P type, the optical luminosity of the peak – coinciding with a major activity of the prompt gamma-ray emission – seems to deviate from any cosmological evolution trend. This fact provides independent confirmation that the prompt physical mechanisms are independent of their location in the Universe. However, the mechanisms of the prompt optical emission are still unclear; with the exception of a few rare cases, the morphology of these peaks is complex and poorly re-sampled.

Acknowledgements

This work was supported by Bologna University Progetti Pluriennali 2003, by grants of CRDF (No. RP1-2394-MO-02), RFBR (No. 04-02-17555, 06-02-08313, 09-02-12053 and 12-02-00743), INTAS (04-78-7366), by the Presidium of the Russian Academy of Sciences Program and by a grant of the President of the Russian Federation for the support of young Russian scientists. S.K. has also been supported by a grant from the Dynasty foundation. G.B. thanks Landau Network-Cenro Volta and the Cariplo Foundation for fellowship and Brera Observatory for hospitality. G.G. also gratefully acknowledges support from Foundatione CARISBO.

References

[1] Fukugita, M., Shimasaku, K. and Ichikawa, T.: Galaxy Colors in Various Photometric Band Systems. *PASP*, **107**, 1995, 945.

[2] Schlegel, D.J., Finkbeiner, D.P. and Davis, M.: Maps of Dust Infrared Emission for Use in Estimation of Reddening and Cosmic Microwave Background Radiation Foregrounds. *ApJ*, **500**, 1998, 525.

[3] Kann, D.A., Klose, S., Zhang, B. et al.: The Afterglows of Swift-era Gamma-ray Bursts. I. Comparing pre-Swift and Swift-era Long/Soft (Type II) GRB Optical Afterglows. *ApJ*, **720**, 2010, 1513–1558.

		$\log T_{\rm peak}$	$\log T_{\rm width}$	$\log T_{\rm opt}$	$\log L_{\rm opt}$	$\log E_{\rm opt}$	$\alpha_{\rm r}$	$\alpha_{\rm d}$	$\log T_{90}$	$\log L_{\rm iso}$	$\log E_{\rm iso}$	α
1		0.23	−0.00	0.01	0.11	0.19	−0.55	0.43	0.19	0.47	0.57	0.12
2		−0.20	−0.26	−0.06	**0.82**	**0.68**	0.16	−0.31	0.19	**0.73**	**0.82**	0.21
3		−0.25	−0.64	0.31	0.74	0.54	−0.33	−0.25	0.02	0.46	0.31	0.44
4	z	−0.03	−0.21	0.25	**0.59**	**0.57**	−0.18	−0.06	0.16	**0.59**	**0.60**	0.15
5		−0.31	−0.44	0.06	**0.82**	**0.67**	0.07	−0.34	0.22	**0.72**	**0.73**	0.31
6		0.72	0.22	−0.64	−0.18	0.03	0.10	0.22	0.31	0.22	0.46	−0.15
7		−0.25	−0.35	0.12	**0.83**	**0.69**	−0.17	−0.20	0.20	**0.74**	**0.75**	0.30
1			0.54	−0.07	**−0.77**	−0.55	0.12	0.03	0.35	−0.51	−0.36	−0.62
2			**0.65**	0.10	−0.21	−0.02	−0.02	−0.11	0.46	−0.39	−0.16	−0.13
3	$\log T_{\rm peak}$		**0.74**	−0.50	−0.37	0.07	−0.20	0.24	−0.67	−0.12	−0.25	0.30
4			**0.76**	0.38	−0.39	0.07	−0.19	0.27	0.02	−0.43	−0.31	−0.37
5			**0.72**	−0.12	−0.35	−0.09	−0.10	0.23	0.10	−0.46	−0.25	−0.15
6			0.64	−0.72	−0.76	−0.54	−0.64	0.20	0.40	−0.36	−0.21	−0.59
7			0.74	−0.03	−0.32	0.01	−0.10	0.20	0.06	−0.40	−0.25	−0.21
1				−0.40	−0.62	**−0.78**	−0.14	−0.08	−0.52	−0.10	−0.32	−0.05
2				0.03	−0.10	0.03	0.04	−0.08	0.23	−0.20	−0.13	−0.09
3	$\log T_{\rm width}$			−0.51	−0.57	−0.27	−0.24	0.59	−0.58	−0.56	−0.21	−0.12
4				0.22	−0.36	−0.02	−0.20	0.36	−0.16	−0.30	−0.27	−0.29
5				−0.20	−0.34	−0.12	−0.09	0.42	−0.09	−0.35	−0.21	−0.18
6				−0.76	−0.70	**−0.81**	**−0.74**	0.10	−0.44	−0.25	−0.52	−0.26
7				−0.11	−0.31	−0.02	−0.13	0.38	−0.13	−0.26	−0.17	−0.21
1					−0.06	0.08	0.19	0.10	0.03	−0.33	−0.27	−0.27
2					−0.07	0.17	−0.25	0.07	−0.05	−0.27	−0.18	0.04
3	$\log T_{\rm opt}$				0.32	0.34	0.30	−0.51	0.48	0.33	0.49	0.11
4					−0.04	0.39	−0.19	0.12	−0.06	−0.19	−0.19	−0.28
5					0.07	0.22	−0.09	−0.22	0.08	−0.11	0.00	0.10
6					0.47	0.49	0.34	−0.29	0.22	−0.16	0.08	0.27
7					0.10	0.28	−0.18	−0.16	0.05	−0.04	0.03	0.06

(continued on the next page)

(cont.)

		$\log T_{\rm peak}$	$\log T_{\rm width}$	$\log T_{\rm opt}$	$\log L_{\rm opt}$	$\log E_{\rm opt}$	$\alpha_{\rm r}$	$\alpha_{\rm d}$	$\log T_{90}$	$\log L_{\rm iso}$	$\log E_{\rm iso}$	α
1						**0.88**	−0.03	0.24	−0.28	0.72	**0.74**	**0.79**
2						**0.88**	0.36	**−0.55**	0.09	**0.77**	**0.79**	0.33
3	$\log L_{\rm opt}$					**0.76**	−0.36	0.09	−0.02	0.69	0.58	0.70
4						**0.77**	0.12	−0.12	0.10	**0.76**	**0.75**	**0.51**
5						**0.85**	0.19	−0.30	0.15	**0.78**	**0.76**	0.47
6						**0.87**	0.83	0.14	−0.42	0.74	0.74	**0.87**
7						**0.83**	−0.04	−0.19	0.15	**0.76**	**0.76**	0.45
1							0.12	0.30	0.10	0.64	**0.76**	0.47
2							0.22	**−0.59**	0.29	**0.66**	**0.73**	**0.54**
3	$\log E_{\rm opt}$						−0.40	0.12	−0.01	**0.83**	0.69	0.69
4							−0.01	0.02	0.17	**0.62**	**0.61**	0.35
5							0.12	−0.30	0.27	**0.70**	**0.74**	0.58
6							0.81	0.13	0.00	0.75	**0.86**	**0.54**
7							−0.15	−0.16	0.23	**0.67**	**0.70**	0.48
1								−0.25	−0.04	−0.32	−0.12	−0.29
2								**−0.60**	−0.02	0.16	0.20	0.08
3								−0.72	0.27	−0.28	−0.20	−0.26
4	$\alpha_{\rm r}$							−0.45	0.06	−0.04	0.07	0.05
5								**−0.56**	0.06	0.12	0.13	0.02
6								0.18	−0.01	0.67	0.84	0.79
7								**−0.60**	0.06	−0.17	−0.09	−0.01
1									−0.04	0.17	0.34	−0.04
2									−0.15	−0.20	−0.23	−0.29
3									−0.45	0.03	0.18	0.05
4	$\alpha_{\rm d}$								−0.28	−0.10	−0.00	−0.23
5									−0.33	−0.22	−0.13	−0.18
6									−0.31	−0.05	0.28	−0.17
7									−0.31	−0.09	−0.04	−0.16
1										−0.40	−0.13	−0.65
2										0.14	0.45	0.28
3										0.48	0.21	−0.24
4	$\log T_{90}$									0.16	0.37	0.14
5										0.25	0.44	0.18
6										−0.48	−0.08	−0.70
7										0.20	0.40	0.17
1											**0.89**	0.68
2											**0.89**	0.41
3											0.70	0.44
4	$\log L_{\rm iso}$										**0.88**	0.47
5											**0.87**	0.44
6											0.82	0.51
7											**0.88**	0.44
1												0.63
2												0.45
3												0.56
4	$\log E_{\rm iso}$											**0.53**
5												**0.50**
6												0.45
7												**0.51**

TABLE 1. Pair correlation coefficients for rest frame parameters. Those shown in bold have correlation coefficients greater than 0.5 and significance better than 1%. 1: P, 2: A, 3: A(U), 4: P+A+A(U), 5: A(U)+A, 6: P-3, 7: [A(U)+3]+A

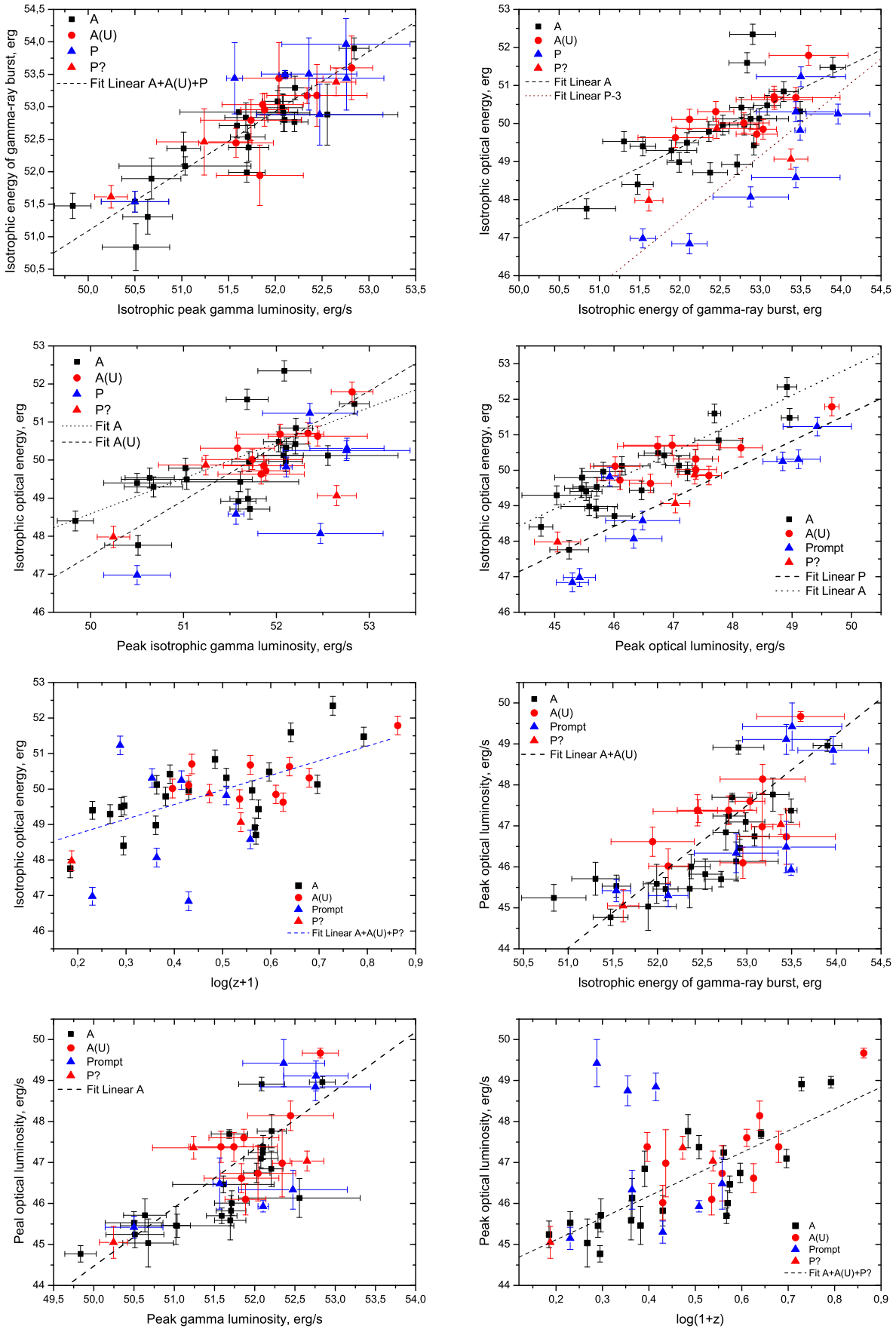

FIGURE 1. Scatter plots of pair correlations between various parameters.

Correlation	*Type*	a	b
$E_{\rm iso} - L_{\rm iso}$	P	1.58 ± 5.60	0.99 ± 0.11
	A	5.04 ± 6.78	0.93 ± 0.13
	A+A(U)+P	5.09 ± 4.31	0.92 ± 0.08
	A+A(U)	7.34 ± 5.67	0.88 ± 0.11
	A+A(U)+P?	8.20 ± 4.91	0.86 ± 0.09
$E_{\rm opt} - L_{\rm opt}$	P	11.62 ± 7.14	0.80 ± 0.15
	A	12.91 ± 4.57	0.80 ± 0.10
	A(U)	28.63 ± 0.43	0.46 ± 0.14
	A+A(U)+P	17.45 ± 4.89	0.69 ± 0.09
	A+A(U)	17.76 ± 3.65	0.69 ± 0.08
	P-3	9.87 ± 8.85	0.83 ± 0.19
	A+A(U)+P?	17.26 ± 3.82	0.70 ± 0.08
$E_{\rm opt} - (z+1)$	A	47.90 ± 0.51	4.26 ± 1.03
	A+A(U)	48.09 ± 0.41	3.89 ± 0.78
	A+A(U)+P	47.81 ± 0.46	4.13 ± 0.93
	A+A(U)+P?	47.92 ± 0.39	4.11 ± 0.75
$E_{\rm iso} - (z+1)$	A	50.84 ± 0.28	3.49 ± 0.58
	A+A(U)+P	51.73 ± 0.31	2.17 ± 0.61
	A+A(U)	51.09 ± 0.28	2.98 ± 0.52
	A+A(U)+P?	51.09 ± 0.26	3.01 ± 0.49
$E_{\rm opt} - T_{\rm width}$	P	53.49 ± 1.22	-3.94 ± 1.04
	P-3	54.28 ± 1.61	-4.45 ± 1.32
$L_{\rm opt} - E_{\rm iso}$	P	-32.52 ± 24.03	1.50 ± 0.45
	A	-32.3 ± 13.2	1.50 ± 0.25
	A+A(U)+P	-30.16 ± 11.95	1.46 ± 0.23
	A+A(U)	-44.11 ± 11.60	1.73 ± 0.22
	A+A(U)+P?	-41.69 ± 11.14	1.69 ± 0.21
$T_{\rm peak} - T_{\rm width}$	A	1.24 ± 0.24	0.51 ± 0.13
	A+A(U)+P	1.00 ± 0.13	0.59 ± 0.08
	A+A(U)	1.22 ± 0.16	0.50 ± 0.09
	A+A(U)+P?	1.16 ± 0.14	0.53 ± 0.08
$*E_{\rm opt} - \alpha_{\rm decay}$	A	48.89 ± 0.36	-1.01 ± 0.32
$E_{\rm opt} - L_{\rm iso}$	A	2.09 ± 12.02	0.93 ± 0.23
	A(U)	-24.50 ± 18.63	1.44 ± 0.36
	A+A(U)+P	2.88 ± 9.55	0.91 ± 0.18
	A+A(U)	-0.39 ± 9.49	0.97 ± 0.18
	A+A(U)+P?	2.80 ± 9.22	0.91 ± 0.18
$E_{\rm opt} - E_{\rm iso}$	P	-20.74 ± 19.69	1.32 ± 0.37
	A	-4.20 ± 11.40	1.03 ± 0.22
	A+A(U)+P	-1.28 ± 10.31	0.97 ± 0.20
	A+A(U)	-3.03 ± 8.91	1.01 ± 0.17
	P-3	-40.95 ± 21.49	1.70 ± 0.41
	A+A(U)+P?	-1.8 ± 9.16	0.98 ± 0.17
$L_{\rm opt} - (z+1)$	A	43.92 ± 0.42	5.41 ± 0.95
	A+A(U)+P	45.03 ± 0.55	3.66 ± 1.17
	A+A(U)	44.03 ± 0.39	5.31 ± 0.79
	A+A(U)+P?	44.05 ± 0.35	5.32 ± 0.73
$L_{\rm iso} - (z+1)$	A	50.28 ± 0.36	2.86 ± 0.77
	A+A(U)+P	50.82 ± 0.32	2.11 ± 0.66
	A+A(U)	50.39 ± 0.29	2.66 ± 0.56
	A+A(U)+P?	50.30 ± 0.28	2.82 ± 0.55
$L_{\rm opt} - Tpeak$	P	52.73 ± 2.03	-3.86 ± 1.24
$L_{\rm opt} - L_{\rm iso}$	A	-27.03 ± 11.95	1.43 ± 0.23
	A+A(U)+P	-29.88 ± 10.01	1.49 ± 0.19
	A+A(U)	-37.96 ± 9.85	1.65 ± 0.19
	A+A(U)+P?	-32.90 ± 9.65	1.55 ± 0.19
$E_{\rm opt} - (z+1)$	A	47.90 ± 0.51	4.26 ± 1.03
	A+A(U)	48.09 ± 0.41	3.89 ± 0.78
	A+A(U)+P	47.81 ± 0.46	4.13 ± 0.93
	A+A(U)+P?	47.92 ± 0.39	4.11 ± 0.75
$*L_{\rm opt} - \alpha_{\rm decay}$	A	46.11 ± 0.46	-0.88 ± 0.35

TABLE 2. Pair correlations for various classes of optical companions with correlation coefficients greater than 0.5 and significances less than 1%. Four columns are linear regression ($a + b \cdot x$) coefficients, derived through unweighted least squares. The stars mark the log-linear correlations, in contrast to the log-log correlations used otherwise.